

See discussions, stats, and author profiles for this publication at: <https://www.researchgate.net/publication/229212666>

# Coatings of PDMS-modified epoxy via urethane linkage: Segmental correlation length, phase morphology, thermomechanical and surface behavior

ARTICLE *in* PROGRESS IN ORGANIC COATINGS · JULY 2009

Impact Factor: 2.36 · DOI: 10.1016/j.porgcoat.2009.02.007

---

CITATIONS

23

---

READS

46

8 AUTHORS, INCLUDING:



**Sangram K. Rath**

Defence Research and Development Organisa...

37 PUBLICATIONS 264 CITATIONS

SEE PROFILE



**Asit Baran Samui**

Institute of Chemical Technology, Mumbai

92 PUBLICATIONS 1,000 CITATIONS

SEE PROFILE



**Shilpa Sawant**

Bhabha Atomic Research Centre

32 PUBLICATIONS 412 CITATIONS

SEE PROFILE

# Structure–Thermomechanical Property Correlations of Highly Branched Siloxane–Urethane Networks

Someshwarnath Pandey, Sangram K. Rath, and Asit. B. Samui\*

Naval Materials Research Laboratory, Shil-Badlapur Road, Addl. Ambernath, Ambernath 421506, Maharashtra, India

## Supporting Information

**ABSTRACT:** A series of  $B_3$  core-terminated highly branched siloxane–urethane polymers was synthesized through the  $A_2 + B_3$  route. Isophorone diisocyanate (IPDI)-terminated polydimethylsiloxane (PDMS) was used as the  $A_2$  unit and triethanol amine as the  $B_3$  core. Size exclusion chromatography (SEC) studies revealed decreasing number-average molecular weights for the branched polymers and increasing tendency toward lower molecular weight species formation with increased proportion of  $B_3$  core in the branched polymers. The degree of branching and fraction of dendritic units, evaluated from  $^1H$  NMR, increased monotonically with increasing  $B_3$  core in the branched polymers. Cross-linked networks of the highly branched polymers were prepared by reaction of the terminal hydroxyl groups with tetraethoxysilane (TEOS) at room temperature. The sol fractions obtained for the networks from solvent extraction studies were consistent with the non-network-forming low molecular weight fractions obtained from the deconvoluted SEC traces. The solubility parameter, Flory–Huggins interaction parameter, and cross-link density of the networks were evaluated from swelling studies. FTIR spectroscopy was used to evaluate the degree of hydrogen bonding of the branched networks. The thermomechanical properties of the networks were evaluated by stress–strain measurements and dynamic mechanical analysis, and the results were correlated with the structural parameters, such as degree of branching, extent of hydrogen bonding, and cross-link density.

## ■ INTRODUCTION

Hyperbranched polymers represent a class of highly branched soluble macromolecules, which has attracted a lot of attention during the past decade. This has resulted in development of several new and simpler synthetic approaches for their preparation.<sup>1–7</sup> Branched polymers containing urethane or urea groups within the backbone are well established as precursors for various polyurethane (PU) resins, foams, and coatings and thus have high industrial importance.<sup>8–13</sup> In general, isocyanate chemistry is thoroughly studied for polymers due to the high versatility and potential to tailor material characteristics by varying the structure of the monomers, monomer combinations, as well as morphology and branch point density control. Hydrogen bonding plays a critical role in this class of materials, and these noncovalent secondary interactions often significantly influence the material properties.<sup>14,15</sup>

Spindler and Fréchet first reported the preparation of high molecular weight hyperbranched polyurethanes using  $AB_2$ -type monomers containing a hydroxyl (A) and two blocked isocyanate groups ( $B_2$ ).<sup>16</sup> Kumar et al. also used an  $AB_2$ -type monomer and reported the preparation of fully aromatic hyperbranched polyurethane from 3,5-dihydroxybenzoylazides using Curtius-type rearrangement reactions.<sup>17</sup> Since the  $AB_x$  approach necessitates rather innovative chemistry approaches due to the high reactivity of the NCO group, researchers resorted to the  $A_2 + B_3$  approach for hyperbranched polyureas and polyurethanes to simplify the process and facilitate work with more commonly available monomers. Thus, hyperbranched polyurethane polyols and polyisocyanates could be synthesized based on conventional raw materials, exploiting the differences in reactivity in an  $A_2 + CB_2$  or  $AA' + CB_2$  (or  $AA' +$

$B'B_2$ ) approach.<sup>18–20</sup> On the basis of the present work, we discuss certain literature reports on the  $A_2 + B_3$  approach to prepare hyperbranched polyurethanes. Sheth et al. reported the preparation of segmented hyperbranched polyurethanes by an oligomeric  $A_2 + B_3$  approach.<sup>21</sup> They used diisocyanate-capped polyethylene oxide or polypropylene oxide as the  $A_2$  units, while oligomeric triamines were used as the  $B_3$  core. The resulting products with degree of branching in the range 30–50% showed microphase-separated morphologies and mechanical properties close to their linear analogues. Unal et al. demonstrated the preparation of segmented, hyperbranched polyurethaneureas using the same approach,<sup>22</sup> where  $A_2$  was an isocyanate end-capped polyether glycol, such as poly-(tetramethylene oxide) glycol (PTMO), and  $B_3$  was an aliphatic triamine. They reported the importance of slow addition of  $A_2$  units onto the  $B_3$  core to control the gelation, structural regularity, and minimization of cyclic species in preparation of branched polyurethanes. Oguz et al. reported the structure development in hyperbranched polymers prepared by the oligomeric method through experimental studies and Monte Carlo simulations.<sup>23</sup> They observed a strong influence of solution concentration on the gel point and the extent of cyclization on the polymers formed. Although there are several such reports on synthesis and characterization of hyperbranched or highly branched polyurethanes and polyureas, studies on further use of end-functionalized polymers to prepare cross-linked networks are limited. Further, in all these

**Received:** April 2, 2011

**Revised:** February 1, 2012

**Accepted:** February 1, 2012

**Published:** February 1, 2012

reports the oligomeric  $A_2$  unit used is either a polyther or a polyester-type polyol capped with an aliphatic or aromatic diisocyanate.

Thus, the objective of the present work is to establish structure–property correlations of networks of end functional highly branched siloxane–urethanes cross-linked with a tetrafunctional cross-linker (TEOS). Hydroxyl end functional highly branched siloxane–urethane polymers were prepared by reacting an isophorone diisocyanate-capped PDMS ( $A_2$ ) unit with a triethanol amine ( $B_3$ ) in different proportions using the oligomeric  $A_2 + B_3$  approach. The degree of branching of the polymers was evaluated by  $^1\text{H}$  NMR using both Frey and Fréchet methods. Heterogeneity in the molar mass distribution of the polymers was evaluated by deconvolution of the GPC traces. The hydroxyl end-functionalized polymers were reacted with tetraethoxy silane (TEOS) at room temperature to prepare cross-linked networks. Swelling studies of the networks were carried out to evaluate the sol–gel fraction and cross-link density. Thermomechanical properties of the networks were evaluated using DMA and stress–strain measurements. FTIR spectroscopy was used to find out the variation of degree of hydrogen bonding of the networks. Structure–thermomechanical property correlation of the networks was carried out in light of the structural parameters evaluated by different techniques.

## MATERIALS AND EXPERIMENTAL DETAILS

**Materials.** Silanol-terminated polydimethyl siloxane ( $M_n \approx 2000$ ) was purchased from Dow Corning India Pvt. Ltd. Isophorone diisocyanate (IPDI), 10% dibutyltindilaurate in toluene (DBTDL), and tetraethoxysilane were purchased from E-Merck and used as received. Triethanolamine (Sigma-Aldrich) was freshly distilled before use. Methyl ethyl ketone (MEK) was purchased from E-Merck and distilled over anhydrous  $\text{K}_2\text{CO}_3$  before use.

**Synthesis.** Synthesis of the highly branched siloxane–urethane polymers was carried out in a two-step process: capping of silanol-terminated PDMS with IPDI to prepare the isocyanate-terminated PDMS prepolymer followed by reaction of the free isocyanate of the isocyanate-terminated PDMS with triethanolamine to prepare the branched polymers.

**Capping of Silanol-Terminated PDMS with Isophorone Diisocyanate.** A 100 g amount of silanol-terminated PDMS was taken in a dry 250 mL capacity round-bottom flask equipped with a magnetic stirrer. The material was demoi-  
sturized under vacuum (50 mmHg) at 100 °C. The flask was cooled to 65 °C, and then 22.2 g of isophorone diisocyanate (OH to NCO molar ratio 1:2) was added along with 2 drops of 10% DBTDL in toluene. The temperature of the mixture was maintained at 70 °C and stirred for 4 h under reduced pressure. The reaction progress was monitored by titrimetry as well as FTIR spectroscopy.

**Synthesis of Highly Branched Siloxane–Urethanes.** The highly branched siloxane–urethanes were prepared by an oligomeric  $A_2 + B_3$  approach. In this method three different branched polymers were prepared by varying the molar ratio of the isocyanate-capped PDMS prepolymer ( $A_2$  moiety) and triethanolamine core moiety ( $B_3$ ) in an  $A_2:B_3$  (molar ratio) of 1:1, 1:1.5, and 1:2. All reactions were carried out in a 3-necked round-bottom flask equipped with an overhead stirrer, an addition funnel, and a nitrogen inlet. Polymerization reactions for preparation of branched polymers were carried out in methyl ethyl ketone (MEK) solutions at room temperature under strong agitation. During the reactions oligomeric  $A_2$

solution was always added dropwise into  $B_3$  solution. In order to prevent gelation the solid content for the reaction was maintained at 15% for all cases. Reaction progress was monitored by tracking the isocyanate content and FTIR spectroscopy through the course of the reaction. After completion of the reaction the solvent was evaporated in a rotary evaporator setup and degassed for 4 h under vacuum to isolate the polymers.

**Hyper 1:1:**  $^1\text{H}$  NMR (500 MHz,  $\text{CDCl}_3$ )  $\delta$  –0.91 (Si– $\text{CH}_3$ ), 0.91–1.04 (– $\text{CH}_3$ ), 1.23–1.90 (– $\text{CH}_2$ ), 2.20 (– $\text{CH}_2$ –C–), 2.76 (N– $\text{CH}_2$ ), 3.52 (–CH–), 3.70 (– $\text{CH}_2$ –O–), 4.09 (–CO–O– $\text{CH}_2$ –), 5.00–6.00 (–NH–).

**Hyper 1:1.5:**  $^1\text{H}$  NMR (500 MHz,  $\text{CDCl}_3$ )  $\delta$  –0.06–0.17 (Si– $\text{CH}_3$ ), 0.91–1.24 (– $\text{CH}_3$ ), 1.24–1.68 (– $\text{CH}_2$ ), 2.50 (– $\text{CH}_2$ –C–), 2.70–2.88 (N– $\text{CH}_2$ ), 3.53–3.58 (–CH–), 3.71 (– $\text{CH}_2$ –O–), 4.10 (–CO–O– $\text{CH}_2$ –), 5.00–6.00 (–NH–).

**Hyper 1:2:**  $^1\text{H}$  NMR (500 MHz,  $\text{CDCl}_3$ )  $\delta$  0.05–0.17 (Si– $\text{CH}_3$ ), 0.85–1.05 (– $\text{CH}_3$ ), 1.13–2.01 (– $\text{CH}_2$ ), 2.69–2.88 (N– $\text{CH}_2$ ), 3.58–3.53 (–CH–), 3.71–3.67 (– $\text{CH}_2$ –O–), 4.10 (–CO–O– $\text{CH}_2$ –), 5.00–6.00 (–NH–).

**Preparation of Cross-Linked Networks.** The synthesized branched siloxane–urethane polymers were used for preparation of cross-linked networks. The hydroxyl-terminated branched polymer was mixed with a stoichiometric amount of tetraethoxysilane (TEOS) in chloroform as solvent with a solid content of 40% (w/v) using dibutyltindilaurate as catalyst (0.4 wt % of branched polymer). The mixture of branched polymer, TEOS, and catalyst in chloroform was then cast in a Teflon mold and allowed to cure at room temperature. In a typical formulation, Hyper 1:1 network was prepared by dissolving 10 g of Hyper 1:1 branched precursor in 25 mL of chloroform followed by addition of 0.49 g of TEOS and 0.04 g of DBTDL and subsequently casting the homogenized mixture in a Teflon mold. The progress of the cross-linking reaction was monitored by tracking the evolution of gel fraction with time.

## CHARACTERIZATION

**Isocyanate Content of Prepolymer.** The isocyanate content of the prepolymer, formed by capping reaction of silanol with IPDI, was measured by titration of the free isocyanate content according to ASTM D 2572-97 standard. According to this method the prepolymer was reacted with an excess of di-*n*-butylamine in toluene for 15 min to ensure completion of the reaction. The excess di-*n*-butylamine was determined by back-titration with standard hydrochloric acid solution.

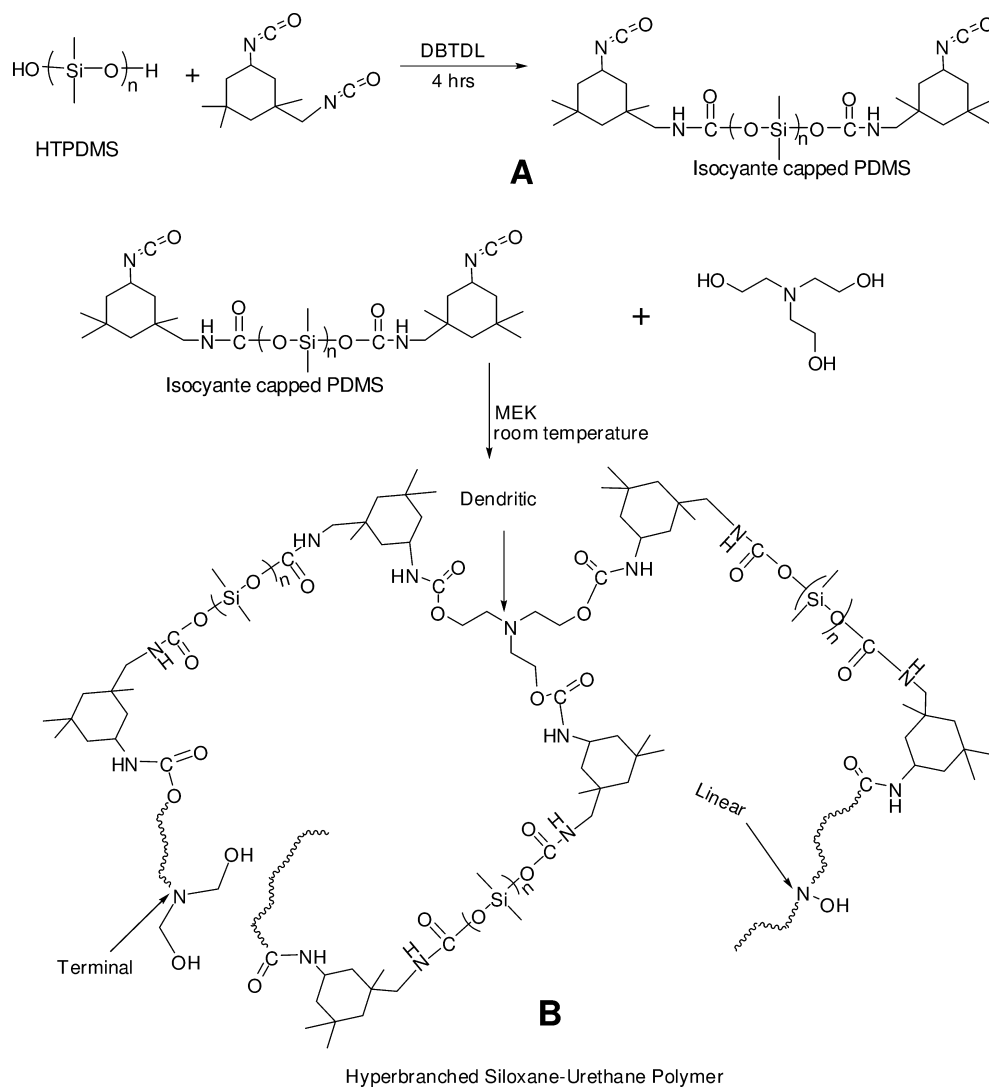
Calculation for NCO content is as follows

$$\text{NCO (\%)} = ((B - V) \times N \times 0.042) / W \times 100$$

where  $B$  is the volume of HCl for titration of the blank (mL),  $V$  is the volume of HCl for titration of the specimen (mL),  $N$  is the normality of HCl, and  $W$  is the specimen weight (g).

**Hydroxyl Value of Branched Polymer.** The hydroxyl values of the  $B_3$  core-terminated branched polymers were determined by refluxing the samples with acetic anhydride in the presence of pyridine. After completion of acetylation, excess acetic anhydride was hydrolyzed with water. The acetic acid formed was titrated with standard potassium hydroxide solution up to the end point. The end point was determined by the inflection point on the titration curve.

**Scheme 1. Capping Reaction of Silanol-Terminated Polydimethyl Siloxane with IPDI and Polycondensation Reaction of IPDI-Capped Siloxane with Triethanol Amine Yielding the Hyperbranched Siloxane–Urethanes**



The hydroxyl value of the polymer sample was calculated from the titer value using the formula given below

$$\text{hydroxyl value (mg/g)} = ((B - A) \times N \times 56.1) / W$$

where  $B$  is the blank reading,  $A$  is the sample reading,  $N$  is the normality of the standard NaOH solution, and  $W$  is the sample weight

**Density.** The density of branched networks was determined by weighing them in air and ethanol using an analytical balance (Mettler AE 200) and a homemade device similar to the Mettler density kit ME-33360 following the equation

$$\rho = \frac{\rho_{\text{Et}} M}{M - M_1} \quad (1)$$

where  $\rho$  is the sample density,  $\rho_{\text{Et}}$  is the density of ethanol,  $M$  is the sample mass in air, and  $M_1$  is its mass in ethanol.

**Sol Fraction Measurements.** The networks thus prepared were extracted in dry THF, and the amount of soluble (uncross-linked) material was evaluated from the weight differences between the final and the initial dry weights.

**Instrumental Characterization.** <sup>1</sup>H NMR analysis of the branched polymers was carried out in a Bruker 500 MHz FT-

NMR spectrometer using CDCl<sub>3</sub> as the solvent at ambient temperature.

GPC measurements of the branched polymers were carried out in a Waters system equipped with a Styragel HT column and a differential refractive index detector using THF as the solvent, and the instrument was calibrated with narrow molecular weight polystyrene standards. The GPC traces were deconvoluted by a Gaussian multipeak procedure available in the ORIGIN v7 program.

Dilute solution viscometry measurements were made with a Schott-Gerate automated viscometer system utilizing a Schotte-Gerate Ubbelohde viscometer tube (bore size 0.46 mm), immersed in a constant temperature water bath at 25 °C.

FTIR spectra of the branched networks were recorded in a Thermo-Nicolet Omnic spectrometer. Each sample was scanned 64 times with a resolution setting of 4 cm<sup>-1</sup> within the range 400–4000 cm<sup>-1</sup>.

The soft segment glass transition temperature ( $T_g$ ), storage modulus ( $E'$ ), and dissipation factor ( $\tan \delta$ ) of the branched networks were determined using a Gabo, Eplexor 100 N, dynamic mechanical analyzer in tensile mode. The temperature



range of analysis was from  $-150$  to  $50$  °C at a frequency of  $1$  Hz, a ramp rate of  $2$  °C  $\text{min}^{-1}$ , and an initial strain of  $0.2\%$ .

Tensile strength measurements of the branched networks were carried using a Hounsfield Universal Testing Machine according to the specification of ASTM D882. The sample size was  $100\text{ mm} \times 10\text{ mm} \times 1\text{ mm}$ , and the crosshead speed was set at  $500\text{ mm/min}$ . For each data point five samples were tested, and the average was recorded.

## RESULTS AND DISCUSSION

**Synthesis.** In the present study the  $A_2 + B_3$  approach has been adopted for synthesis of highly branched siloxane–urethane polymers. The isocyanate-capped PDMS was used as the oligomeric  $A_2$  moiety and the triethanol amine as the core  $B_3$  moiety. The isocyanate-capped material was prepared by end capping of silanol-terminated PDMS with isophorone diisocyanate. The schematic of the capping reaction is given in Scheme 1A. The isocyanate content of the prepolymer was found to be  $3.3\%$  versus the theoretical value of  $3.43\%$ , implying completion of the capping reaction. Further, the prepolymer showed urethane peaks at  $1710\text{ cm}^{-1}$  due to reaction of the hydroxyl groups with isocyanate of IPDI. Unreacted isocyanate was characterized by the appearance of a peak at  $2270\text{ cm}^{-1}$ , while the hydroxyl group of the silanol-terminated PDMS was absent in the prepolymer. This indicated completion of the capping reaction.

Branched polymer synthesis (Scheme 1B) was carried out with a reactant concentration of  $15\%$  to avoid gelation as reported by Unal et al.<sup>22</sup> For preparation of the branched polymers, the  $B_3$  core was always used in excess of the  $A_2$  unit; the lowest molar ratio used was  $1:1$  of  $A_2:B_3$ . In the case of an equimolar ratio of  $A_2$  and  $B_3$  (or in terms of equivalents  $[A]/[B] = 2/3 = 0.67$ ),  $[B]$  was in excess; hence, no gelation was observed. The reaction progress was monitored by isocyanate content measurements for all polymers. The schematic of the curing reaction to prepare the hyperbranched network is given in Scheme 2. Figure 1A shows FTIR spectra of the branched

completion of the condensation reaction. The peaks due to the urethane hard segments are seen around  $3300\text{ cm}^{-1}$  ( $-\text{NH}$  stretching) and a broad band from  $1690$  to  $1710\text{ cm}^{-1}$  ( $-\text{C}=\text{O}$  stretching). Other characteristic absorption peaks are seen at  $1260$  ( $-\text{CH}_3$  bending),  $1020$  and  $1100$  ( $-\text{Si}-\text{O}-\text{Si}-$  stretching), and  $860$  and  $810\text{ cm}^{-1}$  ( $-\text{CH}_3$  rocking of  $-\text{Si}(\text{CH}_3)_2-\text{O}-$ ), attributable to the PDMS soft segment. FTIR spectra thus verified the synthesis and structure of the branched polymers. The intensity of the  $-\text{OH}$  stretching peak (from peak area) is found to increase with increasing  $B_3$  core in the branched polymer. Quantitative evaluation of the hydroxyl content of the branched polymers was carried out by titrimetry, and the values are shown in Table 2. The hydroxyl values of the branched polymers are in the order Hyper  $1:2$  ( $69.7$ ) > Hyper  $1.1:5$  ( $63.4$ ) > Hyper  $1:1$  ( $53.9$ ) and consistent with the FTIR observation of increasing hydroxyl peak intensity with increasing  $B_3$  core content in the branched polymers. However, it must be noted that the increase in hydroxyl value with increasing  $B_3$  core content is not commensurate with the theoretical values based on the stoichiometry of the  $A_2$  and  $B_3$  moieties. This can be attributed to the increasing cyclic species formation with increased core moiety ( $B_3$ ) during  $A_2 + B_3$  polycondensation reactions.<sup>22</sup> Detailed quantification of the cyclic species formation is discussed in the molar mass characterization of the branched polymers by GPC.

The cross-linking reaction of the precursor branched polymers and TEOS catalyzed by  $0.4\text{ wt } \%$  DBTDL (at RT) was monitored by periodic measurement of the gel fraction by solvent extraction with THF. A typical plot for evolution of the gel fraction with time for Hyper  $1:2$  network formation is shown in Figure 2. From the results it is observed that  $80\%$  gel fraction is obtained within a reaction time of  $300\text{ min}$  ( $5\text{ h}$ ). The gel fraction value stabilizes at  $\sim 83\%$  with no further increase in the value even after  $4000\text{ min}$ . The gel fraction values for Hyper  $1:1$  and Hyper  $1.1:5$  networks attained peak values at relatively longer times of  $340$  and  $420\text{ min}$ , respectively.

**Degree of Branching (DB) Determination from  $^1\text{H}$  NMR.** The degree of branching of the branched polymers was calculated using the Fréchet and Frey methods using eqs 2 and 3, respectively<sup>3</sup>

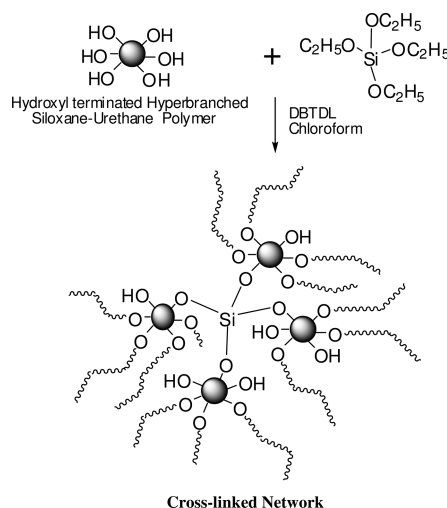
$$\text{DB} = (D + T)/(D + T + L) \quad (2)$$

$$\text{DB} = (2D)/(2D + L) \quad (3)$$

where  $D$  is the peak intensity of dendritic unit,  $T$  is the peak intensity of the terminal unit, and  $L$  is the peak intensity of the linear unit.

$^1\text{H}$  NMR traces of the branched polymers with assignment of dendritic, terminal, and linear protons are given in Figure 3. The fraction of dendritic, linear, and terminal units and DBs were calculated from the corresponding integrated peaks and are given in Table 1. It is observed that with increasing  $B_3$  core in the branched structures both the DB and the fraction of dendritic core increases monotonically. In the case of the  $A_2 + B_3$  reaction, high sensitivity of the DB on the ratio of the monomers as well as on the sequence of the monomer addition has been experimentally observed and simulated.<sup>24,25</sup> The simulations by Schmaljohann<sup>25</sup> showed that at a  $1:1$  ratio of  $A_2/B_3$  a strong difference could be observed depending on the sequence of monomer addition. Applying simultaneous stepwise addition of  $A_2$  and  $B_3$ , a DB of  $0.65$  could be achieved, compared to stepwise addition of  $B_3$  to  $A_2$  solution,

**Scheme 2. Schematic of Preparation of Cross-Linked Siloxane–Urethane Networks from Hydroxyl-Terminated Hyperbranched Siloxane–Urethane with TEOS**



polymers with the magnified  $-\text{OH}$  stretching peak shown in the inset. From the spectra it is observed that the free isocyanate peak at  $2270\text{ cm}^{-1}$  is absent for all samples, implying

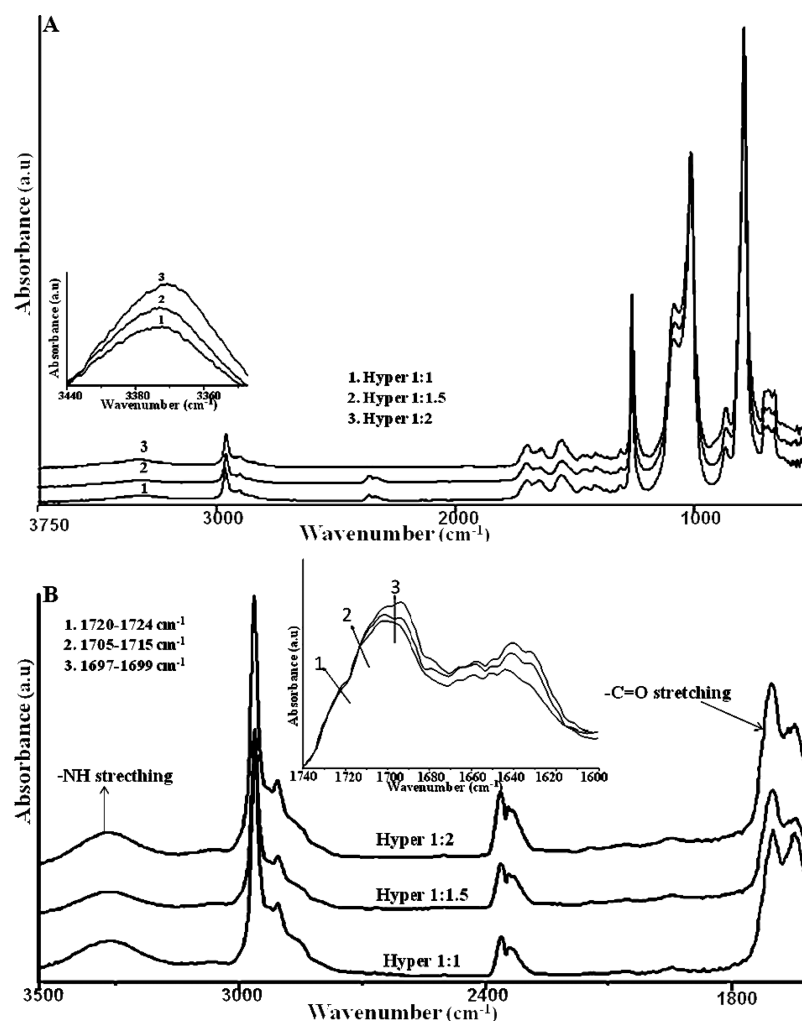


**Figure 1.** (A) FTIR spectra of the branched polymers; (inset) magnified  $\text{--OH}$  stretching region. (B) Partial FTIR spectra of cross-linked branched networks; (inset) magnified  $\text{--C=O}$  stretching region.

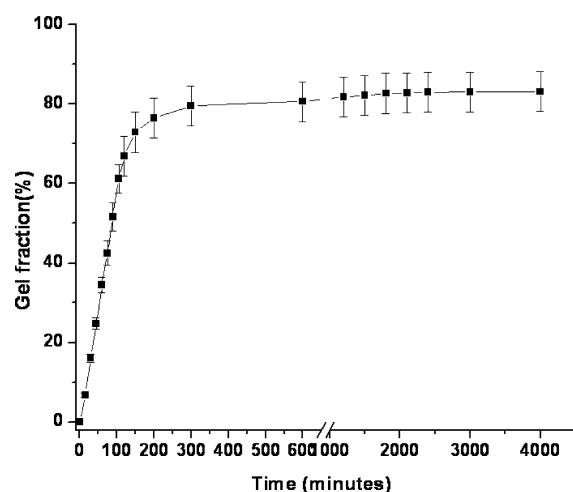


**Figure 2.** Evolution of gel fraction with time during cross-linking of Hyper 1:2 branched polymer with TEOS at RT.

which leads to a DB of 0.91. In the present case, although the slow addition technique has been adopted the DB was found to be in the range 0.5–0.67, implying only highly branched polymer formation. It is thus clear that the benefits of slow addition are not evident in the present case. This could be

attributed to the fact that the  $\text{B}_3$  moiety used here is a hydroxyl functional; hence, its reaction with NCO-terminated  $\text{A}_2$  will be rather slow at room temperature. Therefore, slow or fast addition of  $\text{A}_2$  would not make any difference to the structure of the branched polymers unlike in cases of fast reactions involving an amine-terminated  $\text{B}_3$  moiety.<sup>9,21–23</sup> Besides the equal reactivity of the different functional groups, the low extent of side reactions is crucial for achieving a statistical DB. Cyclization is the most investigated side reaction in  $\text{AB}_x$  or  $\text{A}_2 + \text{B}_y$  polymerization processes.<sup>26–30</sup> Kricheldorf carried out extensive investigations on these structures and developed a cyclization theory in order to account for the deviations of the hyperbranched structures from the cascade theory of Flory.<sup>31</sup> The low DB for the branched polymers in the present case could be attributed to such cyclization possibilities, which is further discussed in the SEC results on the heterogeneous molar mass distribution of the hyperbranched polymers.

**Molar Mass Characterization.** Figure 4 shows the size exclusion chromatogram (SEC) traces of the branched polymers. It is observed that the peak position shifts toward higher retention times with increasing  $\text{B}_3$  core in the branched polymers, implying a decrease in molecular weight. One characteristic feature of all the traces is that the peak shape is not perfectly Gaussian; rather they are skewed toward the right. Thus, the molar mass distribution of the polymers is rather

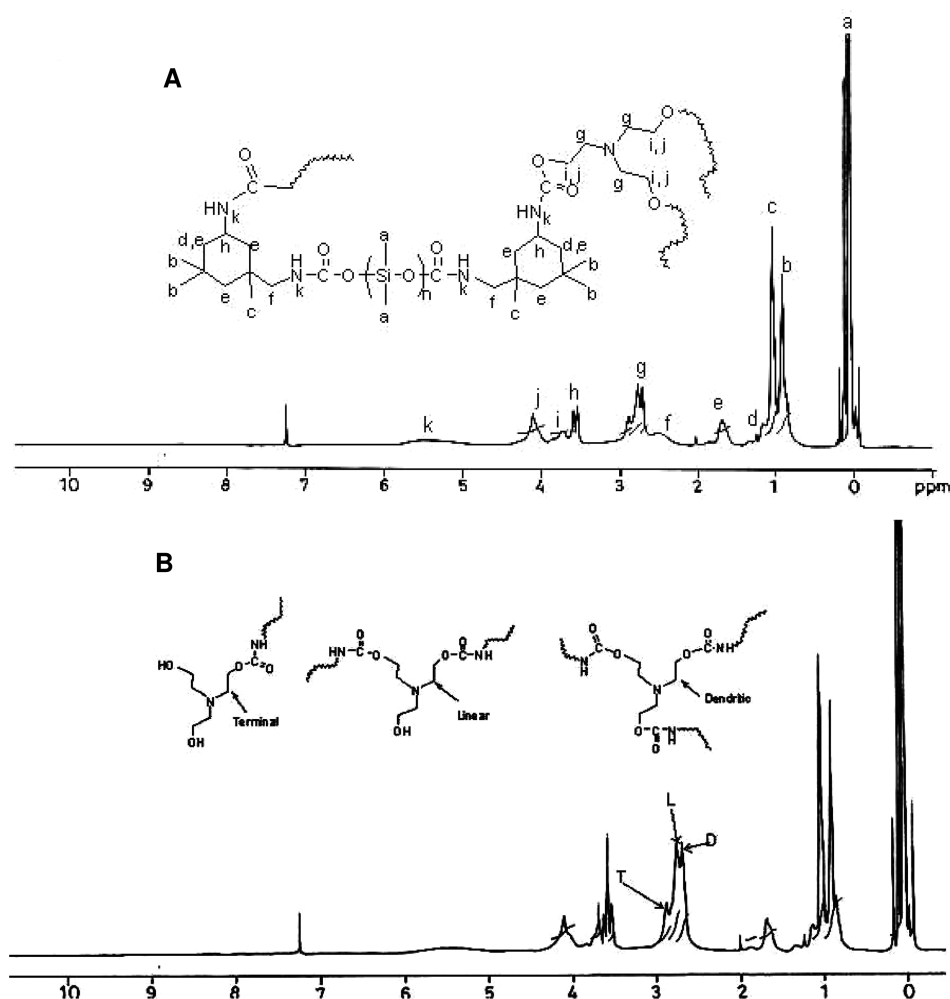


Figure 3. (A)  $^1\text{H}$  NMR trace of Hyper 1:1. (B) Assignment of linear, dendritic, and terminal units of Hyper1:1 from  $^1\text{H}$  NMR trace.

Table 1. Quantification of Structural Units from  $^1\text{H}$  NMR

| sample      | % L | % T  | % D  | DB (Frey) | DB (Frechet) |
|-------------|-----|------|------|-----------|--------------|
| Hyper 1:1   | 52  | 20.4 | 27.3 | 0.47      | 0.51         |
| Hyper 1:1.5 | 51  | 20.2 | 28.4 | 0.48      | 0.52         |
| Hyper 1:2   | 43  | 19.0 | 37.7 | 0.57      | 0.63         |

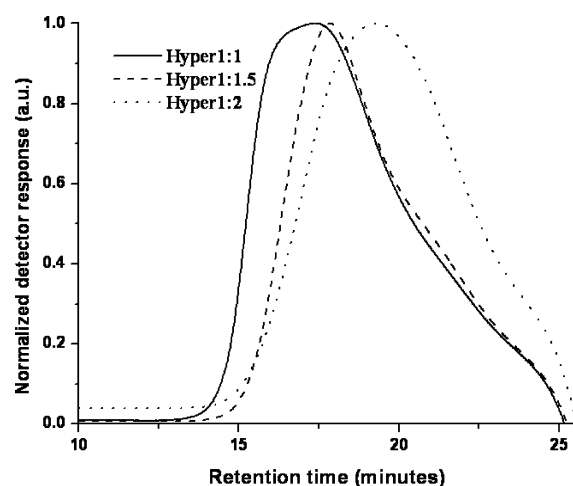


Figure 4. SEC traces of the hyperbranched polymers.

heterogeneous in nature. A definitive presence of low molecular weight fractions might contribute to the broadening of the traces in the higher retention time region corresponding to low molecular weight fractions. As already mentioned, cyclization is the most investigated side reaction in  $\text{AB}_x$  or  $\text{A}_2 + \text{B}_y$  polymerization processes. SEC separation of the broadly distributed samples can reveal important information regarding the distribution of intramolecular ring formation within the complex mixture of branched macromolecule.<sup>3</sup> In order to quantify the molar mass distributions we performed deconvolution of the SEC traces. Figure 5 shows typical deconvoluted spectra of Hyper 1:1 and Hyper 1:2 traces, and detailed parameters of the molar mass distribution are shown in Table 2. From the results we observe that the Hyper 1:1 sample shows three Gaussian bands pertaining to three different molar mass distributions: a very small fraction of high molecular weight species corresponding to the peak molecular weight ( $M_p$ ) of 39 200, the main branched structure with an  $M_p$  of 12 800, and molar masses at a higher retention time corresponding to an  $M_p$  of 590. The molar masses corresponding to the higher retention time of 22 min are attributed to formation of low molecular weight cyclic species formed during the polycondensation reaction. The Hyper 1:1.5 and Hyper 1:2 samples show only two Gaussian bands corresponding to the main branched structure and the cyclic species. The fraction of low molecular weight species, due to the cyclic products, increases

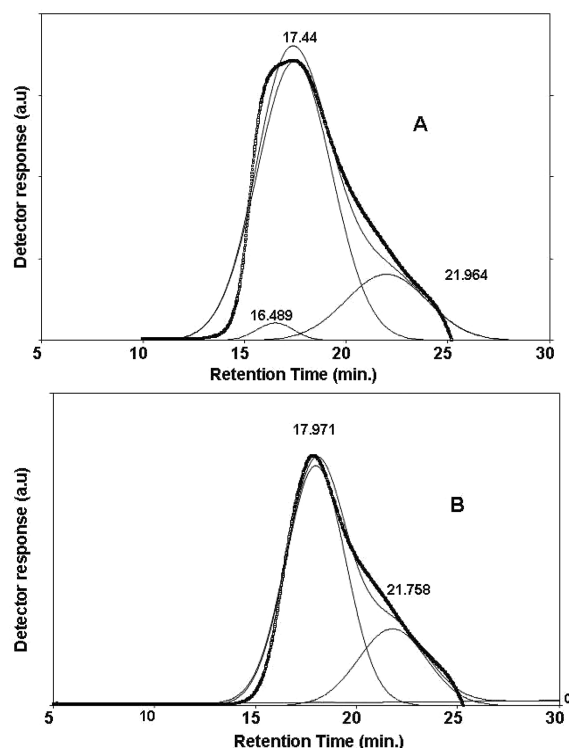


Figure 5. Deconvoluted SEC traces of (A) Hyper 1:1 and (B) Hyper 1:1.5.

Table 2. Molar Mass Distribution of the Branched Polymers from Deconvoluted SEC Traces, Intrinsic Viscosity, and Hydroxyl Value of the Branched Polymers

| sample      | centroids of retention time Gaussian peaks (minutes) | peak molecular weight ( $M_p$ ) g/mol | area (%) | width (min) | intrinsic viscosity (dL/g) | hydroxyl value (mg of KOH/g) |
|-------------|--|---------------------------------------|----------|-------------|----------------------------|------------------------------|
| Hyper 1:1   | 16.48  | 39 200                                | 2.4      | 4.3         |                            |                              |
|             | 17.44  | 12 800                                | 78.3     | 8.6         | 0.135                      | 53.9                         |
|             | 21.75  | 590                                   | 16.3     | 9.4         |                            |                              |
| Hyper 1:1.5 | 17.95  | 7600                                  | 82.9     | 6.8         | 0.092                      | 63.4                         |
|             | 21.9   | 474                                   | 15.1     | 7.9         |                            |                              |
| Hyper 1:2   | 18.2   | 6400                                  | 79.2     | 7.2         | 0.111                      | 69.7                         |
|             | 22   | 380                                   | 18.8     | 7.2         |                            |                              |

with increasing  $B_3$  incorporation into the structures. These findings are consistent with the observation of reported multimodal characteristics of hyperbranched poly(arylester)s prepared by the  $A_2 + B_3$  polycondensation method by two different types of GPC equipment.<sup>32</sup> Furthermore, the decreasing intrinsic viscosity values of the highly branched polymers (Table 2) with increasing  $B_3$  core testifies the increased amount of cyclic species formation and decreasing molecular weight of the highly branched polymers.

**Sol Fraction and Swelling Studies of Highly Branched Networks.** The sol fraction of the branched networks thus prepared (Table 3) is found to increase with increasing  $B_3$  content. The results are consistent with the SEC findings of increasing low molecular weight cyclic species in the networks. It is thus evident that the cyclic species formed during the condensation reactions act as non-network-forming species and

Table 3. Sol Fraction, Flory–Huggins Interaction Parameter, and Cross-Link Density of the Branched Networks Determined from Swelling Studies and the Plateau Modulus of DMA Plots at 25°C

| sample      | sol fraction | $\chi_{MEK}^{(eq)}$ | $V_2$ | $\nu_{swelling}$      | $\nu_{DMA}$          |
|-------------|--------------|---------------------|-------|-----------------------|----------------------|
| Hyper 1:1   | 9.2          | 0.374               | 0.337 | $9.31 \times 10^{-4}$ | $3.1 \times 10^{-3}$ |
| Hyper 1:1.5 | 10.8         | 0.379               | 0.686 | $8.6 \times 10^{-3}$  | $3.7 \times 10^{-3}$ |
| Hyper 1:2   | 12.3         | 0.382               | 0.720 | $3.4 \times 10^{-2}$  |                      |

contribute to the sol fraction. It must be mentioned that pure silanol itself contains some inert dimethylsiloxane cyclics generally present in PDMS samples according to chromatographic measurements.<sup>33</sup> In the present case we found the value to be 6.5%, consistent with the supplier values. Since these species might contribute to the sol fraction values of the networks, the actual sol fraction values are reported after accounting for the cyclic species of the silanol itself.

The cross-link density of the networks was determined using the equilibrium swelling measurements. Cured samples of size 1 mm  $\times$  5 mm  $\times$  5 mm were soaked in dried MEK. After 48 h, the swollen samples were taken out and weighed. The cross-link density was calculated according to the Flory–Rehner equation<sup>34</sup>

$$-[\ln(1 - \nu_2) + \nu_2 + \chi \nu_2^2] = \frac{\rho}{M_c} V_s \left[ \nu_2^{1/3} - \frac{\nu_2}{2} \right] \quad (4)$$

where  $\nu_2$  is the volume fraction of polymer in the swollen mass,  $\rho$  is the density of polymer network sample,  $\chi$  is the Flory–Huggins solvent interaction parameter, and  $V_s$  is the molar volume of the solvent.

The volume fraction of polymer in the swollen network was evaluated using the equation

$$\nu_2 = \frac{w_p}{w_p + w_s \frac{\rho_p}{\rho_s}} \quad (5)$$

where  $w_p$  is the weight of polymer in the swollen mass and  $\rho_p$  and  $\rho_s$  are the density of polymer networks and solvent, respectively.

Following the method proposed by Herrera et al., the Flory–Huggins interaction parameter,  $\chi$ , estimating the interaction energy between the solvent and the polymer network, was calculated using eq 6<sup>35</sup>

$$\ln a_i = \ln \phi_i + (1 - \phi_i) + \chi(1 - \phi_i)^2 \quad (6)$$

where  $a$  is the activity of solvent and  $\phi$  is the volume fraction of solvent in the swollen network. When the sample is immersed in pure solvent, the solvent activity becomes unity and eq 6 can be rewritten as

$$\chi = -\frac{\ln \phi_i + \ln(1 - \phi_i)}{(1 - \phi_i)^2} \quad (7)$$

The values of the interaction parameters obtained (Table 3) are found to increase with increasing core content in the branched networks. The interaction parameters were also calculated from an empirical relationship between the interaction parameter and the solubility parameter of the polymer networks proposed by Bristow and Watson<sup>36,37</sup> (see Supporting Information).



The cross-link density of the networks were then calculated from the Flory–Rehner equation using the  $\chi$  values obtained from eq 7 and are given in Table 3. The results suggest that the cross-link density of the branched networks increases with increasing core content in the network. This is a direct consequence of the increasing hydroxyl end functional concentration with increasing  $B_3$  core incorporation into the branched networks, evident from the increasing hydroxyl value of the branched polymers given in Table 3.

**Hydrogen-Bonding Characteristics from FTIR.** Figure 1B shows the partial FTIR spectra of the highly branched networks with the magnified  $-C=O$  region shown in the inset. In order to evaluate the hydrogen-bonding characteristics of the highly branched networks, we relied on the intensity differences in the broad band of the carbonyl region from 1670 to 1750  $\text{cm}^{-1}$ . It has been established that the strongly hydrogen-bonded carbonyls are responsible for the absorbance at lower wave numbers of 1700–1705  $\text{cm}^{-1}$ .<sup>38</sup> In the present case the same is observed at 1696  $\text{cm}^{-1}$  for the Hyper 1:1 network. The free carbonyl band is noticed at 1726  $\text{cm}^{-1}$ , while the absorbance at 1707  $\text{cm}^{-1}$  corresponds to the loosely hydrogen-bonded carbonyl peak.<sup>39</sup> No discernible trend in the peak position shifts of the various bands with increasing core moiety in the network is noticed. However, with increasing core moiety incorporation into the network, the relative intensity of strongly hydrogen-bonded carbonyl fraction increases, implying a higher degree of phase separation of the networks with increasing  $B_3$  core content.

**Dynamic Mechanical Analysis.** Figure 6A shows the storage modulus ( $E'$ ) vs temperature plot of Hyper 1:1 and Hyper 1:1.5 networks. Measurements on the Hyper 1:2 sample could not be carried out, as the sample could not sustain the dynamic ramp and broke during analysis. The temperature response of  $E'$  could be categorized to four different temperature regimes. The first temperature regime is the glassy plateau which extends from  $-150$  to  $-120$  °C with typically higher  $E'$  values. The glassy plateau is followed by a sharp descent in  $E'$ , corresponding to the glass-transition temperature of the siloxane soft segments, which marks the second temperature regime of  $E'$  response. A transient increase in the modulus is followed in the third temperature regime attributed to cold crystallization of the siloxane segments<sup>40</sup> followed by a drop at  $-50$  °C due to melting of the soft segment crystallites. Finally, the fourth temperature regime is the rubbery plateau which extends from  $-50$  to  $100$  °C.

Sheth et al. carried out extensive studies on the effect of siloxane soft segment molecular weight (SS MW = 7000, 2500, and 900) on the dynamic mechanical properties of hyper-branched siloxane–urethane and urea polymers.<sup>40</sup> They observed crystallization of the PDMS soft segment (SS) for the segmented polyurethane and polyurea copolymers for SS molecular weight of 7000 only.<sup>40</sup> Observation of crystallization of SS in the present case with SS molecular weight of 2000 could be explained on the basis of the differences in hard segment content and the structure of the soft segment. The hard segment contents for the Hyper 1:1 and Hyper 1:1.5 networks are 22% and 25%, respectively, while the systems probed by Sheth et al. have a hard segment content of 30–40%. It is well established that the number of restrictions on the SS increase with higher hard segment content because of higher a degree of phase mixing. Further, the SS used in the present case is a silanol, devoid of any methylene ( $-\text{CH}_2-$ ) groups at the end of PDMS chains, which promotes phase mixing. The

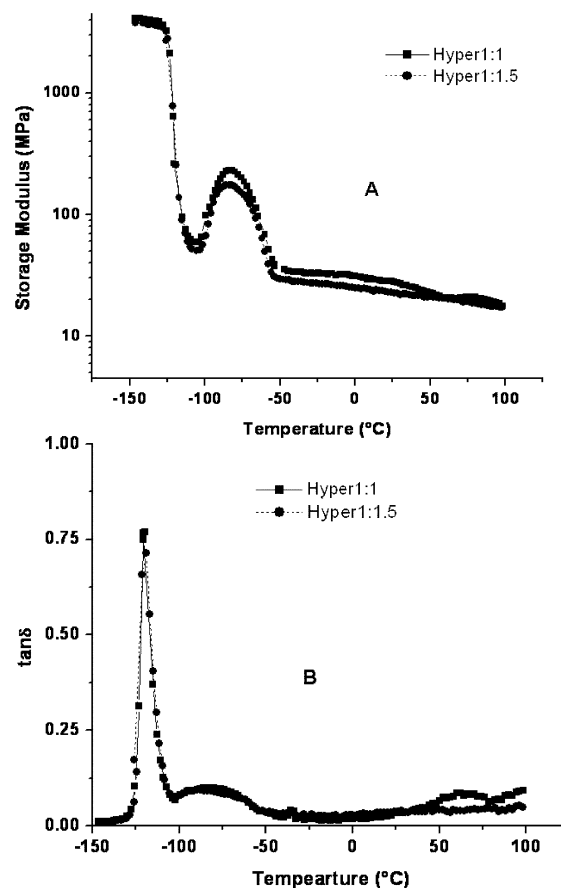


**Figure 6.** DMA plots of the branched networks: (A) storage modulus vs temperature and (B)  $\tan \delta$  vs temperature.

degree of phase separation thus is relatively higher in the present case due to the absence of methylene spacers and lower hard segment content, which in turn leads to observation of SS crystallization.

Predominantly, two transitions pertaining to the glass transition and melting of the siloxane segments have been reported for linear siloxane–urethane polymers, wherein the modulus drop was significantly higher during melting than during  $T_g$ , which is quite reasonable.<sup>41</sup> In the present case the drop in  $E'$  is much higher during the soft segment  $T_g$  compared to the soft segment melting transition. The difference in the temperature dependency could be attributed to the contribution of physical cross-links in linear segmented polyurethanes, while in the present case it is due to the covalently cross-linked chains; the drop in the modulus during the melting process is significantly lower. Hence, the plateau modulus is found to be considerably higher compared to the linear segmented siloxane–urethane polymers. On comparison of  $E'$  response of the networks, one notes that the Hyper 1:1.5 network exhibits a slightly higher plateau modulus compared to the Hyper 1:1 network due to the higher cross-link density.

The dynamic relaxations of the networks are further evident from the  $\tan \delta$  vs temperature plot shown in Figure 6B. From the temperature response of  $\tan \delta$ , two different transitions could be seen. A pronounced soft segment transition is evident from the sharp  $\tan \delta$  peak at  $-120$  °C for Hyper 1:1 network, with a  $\tan \delta$  value (height) of 0.72–0.75. The location of the soft segment  $T_g$  does not change for the Hyper 1:1.5 network, with only a minor depression in the  $\tan \delta$  intensity. This is

followed by a broad mild transition from  $-100$  to  $-50$  °C, with invariant  $\tan \delta$  values for both networks. Comparison of the  $\tan \delta$  profiles of the branched networks with the PDMS-based linear copolymers reported by Sheth et al.<sup>40</sup> provide more insight into the differences in phase separation behavior. The  $T_g$  of the branched networks was found to be  $-120$  °C, versus a value of  $-118$  °C for the linear PDMS polyurethane and polyurea samples with a SS MW of 2500. Further, the  $\tan \delta$  magnitude (peak intensity), a measure of SS mobility, is found to be higher for the networks (0.75) compared to the linear polymers (0.4–0.5). This implies a higher degree of phase separation for the branched networks compared to the linear segmented copolymers and hence a higher extent of phase purity for the PDMS soft segments.

The cross-link density,  $\nu_e$ , the number of moles of elastically effective network chains per cubic centimeter of sample, can be determined from the DMA data using kinetic theory of rubber elasticity. The  $E'$  values at 25 °C were taken to calculate the  $\nu_e$  according to the equation

$$\nu_e = E'/3RT \quad (8)$$

where  $E'$  is the modulus at 25 °C,  $R$  is the universal gas constant, and  $T$  is the temperature in Kelvin.

The cross-link density values obtained from the storage modulus data are given in Table 3. From the results it is observed that the cross-link density values obtained from DMA are higher compared to that obtained from swelling studies. The possible reason for the discrepancy could be that the effect of non-network-forming sol fraction (the cyclic species evaluated from GPC) to the storage modulus is not exactly known. Further, the interference of the sol fraction in evaluation of the swell ratio, volume fraction of the polymer network in the swollen mass, and hence the cross-link density of the networks by swelling studies could not be ruled out.

**Stress–Strain Behavior.** Figure 7 shows a typical stress–strain plot of the branched networks. From the plot it is evident

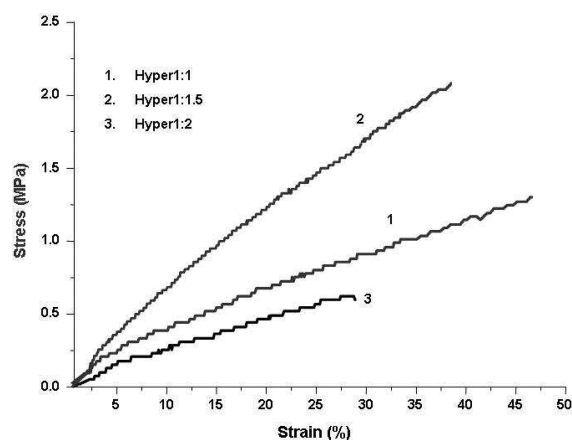


Figure 7. Stress–strain profile of the branched networks.

that Hyper 1:1.5 shows optimum mechanical properties in terms of modulus, tensile strength, as well as elongation at break. On the basis of the cross-link density and degree of hydrogen bonding we expected higher strength and modulus for the Hyper 1:2 network. The counterintuitive poor mechanical properties of the network could be attributed to the presence of a higher amount of non-network-forming low molecular weight species. The latter could act as a plasticizer

and also a stress concentrator, leading to premature failure of the specimen during testing. Interestingly, we find the mechanical properties of the Hyper 1:1.5 network are comparable to siloxane–urethane linear polymers reported with similar lower hard segment concentrations.<sup>41</sup>

## CONCLUSIONS

A series of highly branched siloxane–urethane networks with varying degrees of cross-link densities was prepared by reaction of hydroxyl functional branched precursors with TEOS. The branched polymers were prepared by the oligomeric  $A_2 + B_3$  approach by varying the stoichiometry of IPDI end-capped siloxane ( $A_2$ ) and triethanolamine ( $B_3$ ). Cyclic species formed during preparation of the branched polymers were quantified by deconvolution of SEC traces and found to increase with increasing  $B_3$  content in the highly branched polymers. Characterization of the swelling parameters, hydrogen-bonding characteristics, and thermomechanical properties of the networks were conducted using a range of experimental probes. The extent of strongly hydrogen-bonded fraction and cross-link density of the networks was found to increase with increasing  $B_3$  core content in the branched polymers. DMA studies confirmed the phase-separated morphology of the networks, and a rubbery plateau modulus of 23–25 MPa was observed for the networks at 25 °C. Further studies on the effect of non-network-forming cyclic species, characteristic of the  $A_2 + B_3$  polycondensation approach, on the thermomechanical properties of the networks are underway.

## ASSOCIATED CONTENT

### Supporting Information

The supporting information deals with determination of the Flory–Huggins interaction parameter of the branched networks obtained from swelling studies. This material is available free of charge via the Internet at <http://pubs.acs.org>.

## AUTHOR INFORMATION

### Corresponding Author

\*Tel.: 91-251-2623036. Fax: 91-251-2623004. E-mail: [absamui@gmail.com](mailto:absamui@gmail.com).

### Notes

The authors declare no competing financial interest.

## REFERENCES

- (1) Gao, C.; Yan, D. polymers: from synthesis to applications. *Prog. Polym. Sci.* **2004**, 29 (3), 183–275.
- (2) Jikei, M.; Kakimoto, M. Hyperbranched polymers: a promising new class of materials. *Prog. Polym. Sci.* **2001**, 26 (8), 1233–1285.
- (3) Voit, B. I.; Leder, A. Hyperbranched and Highly Branched Polymer Architectures—Synthetic Strategies and Major Characterization Aspects. *Chem. Rev.* **2009**, 109 (11), 5924–5973.
- (4) Yates, C. R.; Hayes, W. Synthesis and applications of hyperbranched polymers. *Eur. Polym. J.* **2004**, 40 (7), 1257–1281.
- (5) Kim, Y. H. Hyperbranched polymers 10 years after. *J. Polym. Sci., Polym. Chem.* **1998**, 36 (11), 1685–1698.
- (6) Malmström, E.; Hult, A. Hyperbranched Polymers. *J. Macromol. Sci., Rev. Macromol. Chem. Phys.* **1997**, C37 (3), 555–579.
- (7) Fréchet, J. M. J.; Hawker, C. J.; Gitsov, I.; Leon, J. W. Dendrimers and Hyperbranched Polymers: Two Families of Three-Dimensional Macromolecules with Similar but Clearly Distinct Properties. *J. Macromol. Sci., Pure Appl. Chem.* **1996**, A33, 1399.
- (8) Jena, K. K.; Chattopadhyay, D. K.; Raju, K. V. S. N. Synthesis and characterisation of hyperbranched polyurethane-urea coatings. *Eur. Polym. J.* **2007**, 43 (5), 1825–1837.

- (9) Unal, S.; Yilgor, E.; Yilgor, J.; Sheth, J. P.; Wilkes, G. L.; Long, T. E. A New Generation of Highly Branched Polymers: Hyperbranched-, Segmented Poly(urethane urea) Elastomers. *Macromolecules* **2004**, *37* (19), 7081–7084.
- (10) Nasar, A. S.; Jikei, M.; Kakimoto, M. Synthesis and properties of polyurethane elastomers crosslinked with amine-terminated AB<sub>2</sub>-type hyperbranched polyamides. *Eur. Polym. J.* **2003**, *39* (6), 1201–1208.
- (11) Zhang, J.; Hu, C. P. Synthesis, characterization and mechanical properties of polyester-based aliphatic polyurethane elastomers containing hyperbranched polyester segments. *Eur. Polym. J.* **2008**, *44* (11), 3708–3714.
- (12) Czech, P.; Okrasa, L.; Boiteux, G.; Mechin, F.; Ulanski, J. Polyurethane networks based on hyperbranched polyesters: Synthesis and molecular relaxations. *J. Non-Cryst. Solid.* **2005**, *351* (33–36), 2735–2741.
- (13) Feast, W. J.; Rannard, S. P.; Stoddart, A. Selective Convergent Synthesis of Aliphatic Polyurethane Dendrimers. *Macromolecules* **2003**, *36* (26), 9704–9706.
- (14) Yilg r, E.; Burgaz, E.; Yurtsever, E.; Yilg r,  . Comparison of hydrogen bonding in polydimethylsiloxane and polyether based urethane and urea copolymers. *Polymer* **2000**, *41*, 849–857.
- (15) Yilg r, E.; Yilg r,  . Hydrogen bonding: a critical parameter in designing silicone copolymers. *Polymer* **2001**, *42*, 7953–7958.
- (16) Spindler, R.; Jean, M.; Fr chet, J. Synthesis and characterization of hyperbranched polyurethanes prepared from blocked isocyanate monomers by step-growth polymerization. *Macromolecules* **1993**, *26* (18), 4809–4813.
- (17) Kumar, A.; Ramakrishnan, S. Hyperbranched polyurethanes with varying spacer segments between the branching points. *J. Polym. Sci., Part A: Polym. Chem.* **1996**, *34*, 839–848.
- (18) Bruchmann, B.; Schrepp, W. A simple and convenient synthetic strategy towards hyperbranched polyurea-urethanes. *e-Polym.* **2003**, [no. 014].
- (19) Gao, C.; Yan, D. A<sub>2</sub> + CB<sub>n</sub> Approach to Hyperbranched Polymers with Alternating Ureido and Urethano Units. *Macromolecules* **2003**, *36* (3), 613–620.
- (20) Hanselmann, R.; H lter, D.; Frey, H. Hyperbranched Polymers Prepared via the Core-Dilution/Slow Addition Technique, Computer Simulation of Molecular Weight Distribution and Degree of Branching. *Macromolecules* **1998**, *31* (12), 3791–3810.
- (21) Sheth, J. P.; Unal, S.; Yilgor, E.; Yilgor, I.; Beyer, F. L.; Long, T. E.; Wilkes, G. L. A comparative study of the structure–property behavior of highly branched segmented poly(urethane urea) copolymers and their linear analogs. *Polymer* **2005**, *46*, 10180–10190.
- (22) Unal, S.; Oguz, C.; Yilgor, E.; Gallivan, M.; Long, T. E.; Yilgor, I. Understanding the structure development in hyperbranched polymers prepared by oligomeric A<sub>2</sub>+B<sub>3</sub> approach: comparison of experimental results and simulations. *Polymer* **2005**, *46* (13), 4533–4543.
- (23) Oguz, C.; Gallivan, M. A.; Cakir, S.; Yilgor, E.; Yilgor, I. Influence of polymerization procedure on polymer topology and other structural properties in highly branched polymers obtained by A<sub>2</sub> + B<sub>3</sub> approach. *Polymer* **2008**, *49* (5), 1414–1424.
- (24) Unal, S.; Lin, Q.; Mourey, T. H.; Long, T. E. Tailoring the Degree of Branching: Preparation of Poly (ether ester)s via Copolymerization of Poly(ethylene glycol) Oligomers (A<sub>2</sub>) and 1,3,5-Benzenetricarbonyl Trichloride (B<sub>3</sub>). *Macromolecules* **2005**, *38* (8), 3246–3254.
- (25) Schmaljohann, D.; Voit, B. Kinetic Evaluation of Hyperbranched A<sub>2</sub> + B<sub>3</sub> Polycondensation Reactions. *Macromol. Theory Simul.* **2003**, *12* (9), 679–689.
- (26) Gooden, J. K.; Gross, M. L.; Mueller, A.; Stefanescu, A. D.; Wooley, K. L. Cyclization in Hyperbranched Polymer Syntheses Characterization by MALDI-TOF Mass Spectrometry. *J. Am. Chem. Soc.* **1998**, *120* (38), 10180–10186.
- (27) Dusek, K.; Somvarsky, J.; Smrekova, M.; Simansiek, W. J.; Wilezek, Z. Role of cyclization in the degree-of- polymerization distribution of hyperbranched polymers Modelling and experiments. *Polym. Bull. (Berlin)* **1999**, *42*, 489–496.
- (28) Park, D.; Feast, W. J. Synthesis, Structure, and Properties of Hyperbranched Polyesters Based on Dimethyl 5-(2-Hydroxyethoxy) isophthalate. *Macromolecules* **2001**, *34* (7), 2048–2059.
- (29) Chikh, L.; Tessier, M.; Fradet, A. NMR and MALDI-TOF MS study of side reactions in hyperbranched polyesters based on 2,2bis(hydroxymethyl)propanoic acid. *Polymer* **2007**, *48* (7), 1884–1892.
- (30) Jaumann, M.; Rebrov, E. A.; Kazakova, V. V.; Muzafarov, A. M.; Goedel, W.; M ller, M. Hyperbranched Polyalkoxysiloxanes via AB<sub>3</sub>-Type Monomers. *Macromol. Chem. Phys.* **2003**, *204* (7), 1014–1026.
- (31) Kricheldorf, H. R. Polycondensation of ‘a – b<sub>n</sub>’ or ‘a<sub>2</sub> + b<sub>n</sub>’ Monomers - A Comparison. *Macromol. Rapid Commun.* **2007**, *28*, 1839–1870.
- (32) Lin, Q.; Long, T. E. Polymerization of A<sub>2</sub> with B<sub>3</sub> Monomers: A Facile Approach to Hyperbranched Poly(aryl ester)s. *Macromolecules* **2003**, *36* (26), 9809–9816.
- (33) L Lorente, M. A.; Andrady, A. L.; Mark, J. E. Model networks of end-linked polydimethylsiloxane chains. XI. Use of very short network chains to improve ultimate properties. *J. Polym. Sci.: Polym. Phys. Ed.* **1981**, *19*, 621–630.
- (34) Flory, P.; Rehner, J. Statistical Mechanics of Cross – Linked Polymer Networks II. Swelling. *J. Chem. Phys.* **1943**, *11*, 521.
- (35) Herrera-Aloonso, J. M.; Marand, E.; Little, J.; Cox, S. S. Polymer clay/nanocomposites as VOC barrier materials and coatings. *Polymer* **2009**, *50*, S744–S748.
- (36) Gulke, E. A. In *Solubility parameter values: polymer handbook*, 4th ed.; Brandrup, J., Immergut, E. H., Grulke, E. A., Eds.; John Wiley & Sons, Inc.: New York, 1999.
- (37) Bristow, G. M.; Watson, W. F. Cohesive energy densities of polymers. Part 1—Cohesive energy densities of rubbers by swelling measurements. *Trans. Faraday Soc.* **1958**, *54*, 1731.
- (38) Pongkitwitoon, S.; Hern ndez, R.; Weksler, J.; Padsalgikar, A.; Choi, T.; Runt, J. Temperature dependent microphase mixing of model polyurethanes with different intersegment compatibilities. *Polymer* **2009**, *50*, 6305–6311.
- (39) Choi, T.; Weksler, J.; Padsalgikar, A.; Runt, J. Microstructural organization of polydimethylsiloxane soft segment polyurethanes derived from a single macrodiol. *Polymer* **2010**, *51*, 4375–4382.
- (40) Sheth, J. P.; Aneja, A.; Wilkes, G. L.; Yilgor, E.; Atilla, G. E.; Yilgor, I.; Beyer, F. L. Influence of system variables on the morphological and dynamic mechanical behavior of polydimethyl siloxane bases segmented polyurethane and polyurea copolymer: a comparative perspective. *Polymer* **2004**, *45*, 6919–6932.
- (41) Yilgor, I.; Eynur, T.; Yilgor, E.; Wilkes, G. L. Contribution of Soft segmented entanglement on the tensile property of silicone–Urea copolymers with low hard segment contents. *Polymer* **2009**, *50*, 4432–4437.